

Rac GTPase isoform-specific regulation of NADPH oxidase and chemotaxis in murine neutrophils *in vivo*: Role of the C-terminal polybasic domain

Akira Yamauchi*[‡], Christophe C. Marchal*, Jason Molitoris*, Nancy Pech*, Ulla Knaus[♦], Jason Towe[†], Simon J. Atkinson^{†‡} and Mary C. Dinauer*^{#§¶}

*Herman B Wells Center for Pediatric Research, Departments of Pediatrics (Hematology/Oncology),
[†]Medicine (Nephrology), [‡]Biochemistry and Molecular Biology, # Microbiology/Immunology and
[§]Medical and Molecular Genetics, James Whitcomb Riley Hospital for Children, Indiana University
School of Medicine, Indianapolis, Indiana 46202; [♦]Department of Immunology, The Scripps Research
Institute, La Jolla, California 92037; [‡]Current address: Research Center for Advanced Science and
Technology, The University of Tokyo, Tokyo, Japan 153-8904; [♦]Department of Immunology, The
Scripps Research Institute, La Jolla, California 92037

¶Corresponding Author:
Mary C. Dinauer, M.D, Ph.D.
Cancer Research Institute
1044 W. Walnut Street, R4 402C
Indianapolis, IN 46202
Tel: 317-274-8645; Fax: 317-274-8679
E-mail: mdinauer@iupui.edu

Key words:

Running title: Rac polybasic domain mediates isoform-specific functions

Abstract

The Rho family GTPase Rac acts as a molecular switch for signal transduction to regulate various cellular functions. Mice deficient in the hematopoietic-specific Rac2 isoform exhibit agonist-specific defects in neutrophil chemotaxis and superoxide production, despite expression of the highly homologous Rac1 isoform. To examine whether functional defects in *rac2*^{-/-} neutrophils reflect effects of an overall decrease in total cellular Rac or an isoform-specific role for Rac2, retroviral vectors were used to express exogenous Rac1 or Rac2 at levels similar to endogenous. In *rac2*^{-/-} neutrophils differentiated from transduced myeloid progenitors *in vitro*, increasing cellular Rac levels by expression of either exogenous Rac1 or Rac2 increased fMLP- or phorbol ester-stimulated NADPH oxidase activity. Of note, placement of an epitope tag on N-terminus of Rac1 or Rac2 blunted reconstitution of responses in *rac2*^{-/-} neutrophils. In *rac2*^{-/-} neutrophils isolated from mice transplanted with Rac-transduced bone marrow cells, superoxide production and chemotaxis were fully reconstituted by expression of exogenous Rac2, but not Rac1. A chimeric Rac1 protein in which the Rac1 C-terminal polybasic domain, which contains 6 lysines or arginines, was replaced with that of the human Rac2 polybasic domain containing only three basic residues, also reconstituted superoxide production and chemotaxis, whereas expression of a Rac2 derivative in which the polybasic domain was replaced with that of Rac1 did not, and also resulted in disoriented cell motility. Thus, the composition of the polybasic domain is sufficient for determining Rac isoform specificity in the production of superoxide and chemotaxis in murine neutrophils *in vivo*.

Introduction

Neutrophils are important effector cells in the host response to bacterial and fungal pathogens and are endowed with chemotactic and microbicidal functions that are activated by signal transduction pathways downstream of receptors for inflammatory and microbial stimuli (1). Migration from blood vessels to inflamed sites is initiated by various chemoattractants including chemokines secreted by host cells and by bacterial products such as fMLP. Superoxide produced by the neutrophil NADPH oxidase is the precursor to toxic reactive oxidants important for normal microbial killing.

Rac GTPases, members of the Rho family of small GTPases, play a central role in regulating neutrophil chemotaxis, superoxide production, and other neutrophil functions (2). Rho GTPases act as molecular switches in signaling pathways, alternating between activated GTP-bound and inactive GDP-bound states. In unstimulated cells, the GDP-bound form of Rac is bound to Rho guanine-nucleotide dissociation inhibitor (Rho-GDI) which inhibits nucleotide exchange and maintains Rac-GDP in the cytoplasm. Upon stimulation, Rac translocates to the membrane where agonist-activated guanine nucleotide exchange factors mediate the exchange of GDP for GTP, resulting in a conformational change that permits Rac binding to downstream target proteins (3). Rac has three isoforms, the ubiquitously expressed Rac1, a hematopoietic cell-specific isoform Rac2, and Rac3 which appears to be expressed in a variety of tissues but not phagocytes (4-8). The amino acid sequence of murine Rac1 is identical to human Rac1, and murine Rac2 differs by only two amino acids from human Rac2, with a conservative substitution of aspartate instead of glutamate at position 148 and a proline instead of an alanine at position 188 (5,6). Rac1 and Rac2 have 92% identical amino acid sequences. These two isoforms have an identical effector domain (amino acids 26 - 45), which is a critical site of interaction with both guanine nucleotide exchange factors and downstream protein targets. However, long-range effects exerted by distant isoform-divergent amino acids may alter the flexibility of the effector domain to produce different affinities of Rac1 and Rac2 for these proteins (9). The greatest sequence divergence between Rac1 and Rac2 is in the C-terminal polybasic domain (residues 183 - 188), which is adjacent to a prenylated cysteine residue that can insert into cellular membranes. Rac1 has six adjacent basic residues in the

polybasic domain (KKRKRK) whereas Rac2 has only three basic residues interspersed by neutral amino acids (RQQKRA/P) (Fig. 1a). The polybasic domain mediates differential localization of overexpressed Rac1 and Rac2 to fibroblast and epithelial cell membranes (10), and contributes to differential interactions with at least one downstream target of activated Rac GTPases, the serine-threonine kinase PAK1 (11).¹

Studies in murine Rac2-deficient neutrophils and neutrophils from a patient with a dominant-negative mutation in Rac2 suggest that this isoform is essential for normal neutrophil function (8,12-15). Although murine neutrophils have similar amounts of Rac1 and Rac2 (8), genetic deletion of Rac2 results in severely impaired F-actin polymerization and chemotaxis in response to chemoattractants, decreased L-selectin-mediated adhesion, and reduced superoxide production in response to fMLP, phorbol ester, and IgG opsonized sheep red blood cells (8,12,15). Heterozygous *rac2*^{+/-} murine neutrophils have intermediate activity between *rac2*^{+/+} and *rac2*^{-/-} neutrophils in F-actin formation, chemotaxis, and superoxide production (8). In human neutrophils, which have predominantly Rac2, (16) expression of a dominant-negative Rac2 results in cellular defects similar to those seen in *rac2*^{-/-} murine neutrophils (13,14). Although Rac1-null murine neutrophils also exhibit decreased actin cytoskeleton assembly and a modest decrease in directed migration, superoxide production is normal in contrast to Rac2-null counterparts (17). These findings suggest that Rac1 and Rac2 play distinct roles in regulating neutrophil functions. Alternatively, the defects in Rac2-deficient neutrophils could reflect effects of an overall reduction in cellular Rac levels.

The goal of the current study was to examine whether the impaired functions of Rac2-null neutrophils result from a relative cellular deficiency of total Rac or an isoform-specific role for Rac2 that is mediated by specific sequences. Retroviral vectors were used to express exogenous Rac1 or Rac2 in *rac2*^{-/-} neutrophils at levels similar to endogenous. Increasing Rac levels by expression of either exogenous Rac1 or Rac2 enhanced NADPH oxidase activity in *rac2*^{-/-} neutrophils differentiated *in vitro* with growth factors. However, we found that only expression of exogenous Rac2, but not Rac1, fully reconstituted defects in NADPH oxidase activity and chemotaxis in neutrophils harvested from *rac2*^{-/-}

mice transplanted with transduced *rac2*^{-/-} marrow cells. This result could be recapitulated using a derivative of Rac1 in which the polybasic domain was substituted with the corresponding region from human Rac2, and conversely, expression of Rac2 chimeric for the polybasic Rac1 domain failed to rescue defects in *rac2*^{-/-} neutrophils, and resulted in disoriented motility. Thus, the polybasic domain is sufficient to confer isoform-specific Rac functions in regulating neutrophil chemotaxis and NADPH oxidase activity.

Methods

Reagents and buffers

A polyclonal Rac2 antibody was previously raised in rabbits (18) and a mouse mAb against Rac1 was purchased from Upstate Biotechnology (Lake Placid, NY). A rabbit polyclonal for p38MAPK was obtained from Cell Signaling Inc. PBS (pH 7.2), ddH₂O, Glycerol, alpha MEM and IMDM medium, penicillin, streptomycin and HEPES (125mM, pH 7.5) were from Life Technologies (Grand Island, NY). Fetal calf serum (FCS) was from Hyclone laboratory (Logan UT). Rat SCF, murine IL-6, and murine IL-3 were from Peprotech (Rocky Hill, NJ), human MDGF and human G-CSF were from Amgen. CH-296 was from Takara Bio (Otsu, Japan). Other chemicals were purchased from Sigma (St. Louis, MO) unless otherwise stated. Buffers used in this study included PBS with 0.9mM CaCl₂, 0.5mM MgCl₂, and 7.5mM glucose (PBSG), Triton IPB lysis buffer (20mM Tris-Cl pH 8.0, 150mM NaCl, 1mM EDTA, and 1% Triton X-100, 20ug/ml chymostain, 2mM PMSF, 10uM leupeptin, and 1mM 4-(2-aminoethyl benzenesulfonyl fluoride). All reagents are endotoxin-free grade. 96-well plates were from Becton Dickinson (Franklin Lakes, NJ).

Mice

Mice were maintained under specific pathogen-free conditions. Wild type (WT) mice used in this study were 8-10 week old male or female C57/B16J mice purchased from Jackson Laboratory Inc. *Rac2*^{-/-} mice were previously generated (15) by targeted homologous recombination to disrupt the *Rac2* gene. *Rac2*^{-/-} mice used here were 8-10 week old male or female mice that had been backcrossed onto the C57/B16J for more than 11 generations.

Retroviral vectors for expression of Rac proteins

An MSCV retroviral backbone with a linked expression cassette for puromycin-*N*-acetyltransferase (PAC) (19), MSCV-pac, was a kind gift from R. Hawley (American Red Cross, Rockville, MD). The MIEG3 retroviral vector was derived from the MSCV series, and contains an internal

ribosome entry sequence (IRES) linked to a cDNA for the enhanced green fluorescent protein (EGFP) instead of an antibiotic-resistance expression cassette (13). Murine Rac1 and Rac2 cDNA's flanked by BamHI and XbaI restriction sites were originally generated using RT-PCR from RNA prepared from the RAW 264.7 mouse macrophage cell line. The flanking restriction sites were changed to XhoI, along with creation of a Kozak sequence at the initiator ATG, using oligonucleotide primers and PCR, and cloned into the XhoI site in MSCV-Pac and MIEG3 (Fig. 1b). The murine Rac1 or Rac2 cDNA's with an N-terminal hemagglutinin (HA) or FLAG epitope tag (13,20), respectively, were also cloned into MSCV-pac (Fig. 1b). The human Rac1 cDNA in which the Rac2 polybasic domain was replaced with that of Rac1 (Rac1-2) and the human Rac2 cDNA in which the polybasic domain was replaced with that of Rac1 (Rac2-1) were previously described (11). PCR was used to place EcoRI and XhoI linkers at the 5' and 3' ends, respectively, and each was subcloned into the corresponding sites in MIEG3 (Fig 1). Details of oligonucleotide primers used for PCR amplications are provided upon request. For all PCR-amplified cDNAs, DNA sequencing was performed to verify the fidelity of amplification. Vector plasmids were transfected using calcium phosphate into ecotropic Phoenix packaging cells (provided by Gary Nolan, Stanford University; ATCC # SD3444) and retroviral vector supernatants collected in alpha-MEM with 20% FCS.

Transduction of murine bone marrow cells with retroviral vectors for expression of Rac proteins,

Retroviral transduction of WT or *rac2*^{-/-} murine BM was generally as previously described (21), with the following modifications. Three days following injection of 150 mg/kg 5-fluorouracil (5-FU) into bone marrow (BM) donors, BM cells were taken from femurs and tibias by flushing with alpha-MEM. The day of BM harvest was considered Day 0. BM cells were pelleted and resuspended in 10ml of red blood cell lysis solution (155mM NH₄Cl, 10mM KHCO₃, 100μM EDTA in H₂O, pH7.4) in each tube, and kept at room temperature for 3min. Cells were then centrifuged and resuspended in either TD medium A (alpha-MEM with 20% serum, 100 ng/ml rat SCF, 100 ng/ml human MDGF, 100 ng/ml human G-SCF and 2% penicillin/streptomycin) or TD medium B (alpha-MEM with 20% serum, 100

ng/ml rat SCF, 100 units/ml human IL-6 and 2% penicillin/streptomycin) for pre-stimulation for 48 hours. On day 2, 3, and 4, cells were transduced every 24 hours with retrovirus supernatant on 6-well non-treated culture plates that were coated with CH296 ($4 \mu\text{g}/\text{cm}^2$) by overnight incubation at 4C° prior to virus infection. For each round of transduction, cells in suspension were spun down, resuspended in fresh retrovirus supernatant containing either TD medium A or B and returned to the corresponding well and incubated for 24 hours. MSCV-pac vectors were used to transduce cells for *in vitro* differentiation in the presence of puromycin, and MIEG3 vectors were used to transduce cells that were sorted for EGFP fluorescence and transplanted into lethally irradiated recipient mice. There was no difference between these TD medium A or B in either the transduction efficiency or subsequent *in vitro* differentiation and functional assays. Medium without virus was used for mock transduction. On day 5, the combined suspended and adherent cells were collected using Cell Dissociation Buffer (Gibco) and then differentiated *ex vivo* or sorted prior to transplantation into lethally irradiated recipients.

In vitro differentiation of granulocytes following retroviral transduction of murine bone marrow

Neutrophils were differentiated *in vitro* from mock transduced or transduced BM cells by culturing in alpha-MEM with 20% serum, 50 IU/ml murine IL-3, 0.3 ng/ml (=30IU/ml) human G-SCF, and 2% penicillin/streptomycin in T75 flasks. Every other day (on day 6, 8, 10, 12, and 14 post harvest) cell number was counted, and cell density was adjusted to 5×10^5 cells/ml using fresh differentiation media. On day 8 through day 12, cells were selected by adding $2 \mu\text{g}/\text{ml}$ puromycin and by day 12, all mock-transduced cells exposed to puromycin had died. On day 14, cells were harvested for NADPH oxidase assays, using either transduced cells selected with puromycin or mock-transduced cells cultured in the absence of puromycin. Diff-Quik stained cytopins on day 14 showed 80 - 90% mature neutrophils, with no differences seen between WT, Rac2-null, or Rac-transduced cells. The fraction of Gr-1 positive cells as analyzed by flow cytometry was also similar between different groups. Cell lysate was prepared on day 14- 16 for SDS-PAGE and Western blotting.

Transplantation of retrovirus-transduced murine bone marrow cells

To generate neutrophils differentiated *in vivo* from MIEG vector-transduced BM cells, EGFP positive cells were selected on day 5 of the transduction protocol by sorting with a FACStar instrument (Becton Dickinson) and $0.5 - 1.0 \times 10^6$ sorted cells were injected via tail vein into Rac2-null mice that had been irradiated with 1100 cGy (split dose). Following hematopoietic recovery, neutrophils from peripheral blood and BM were assessed by flow cytometry for EGFP marking at four to six weeks after transplantation. Neutrophils were then purified from BM as previously described (12,15) for analysis of NADPH oxidase activity and motility. In some experiments, BM from mice transplanted with sorted, MIEG vector-transduced *rac2*^{-/-} cells were used for secondary transplants into additional 1100cGy-irradiated *rac2*^{-/-} mice to generate additional *in vivo* differentiated neutrophils expressing exogenous Rac. For *rac2*^{-/-} controls, a group of *rac2*^{-/-} mice were transplanted in parallel with freshly isolated *rac2*^{-/-} BM and used as a source of *rac2*^{-/-} neutrophils in subsequent functional assays. However, NADPH oxidase activity and chemotaxis in neutrophils harvested from these mice were no different from neutrophils harvested from non-transplanted *rac2*^{-/-} mice.

Immunoblotting

Preparation of neutrophil lysates, SDS-PAGE, and immunoblotting were performed as described (12,15,22). Briefly, neutrophils differentiated *in vitro* or purified from BM were treated with diisopropylphosphofluoridate prior to lysis with IP buffer (1% Triton X-100, 150 mM NaCl, 10 mM Tris-Cl, 1 mM EDTA, 1 mM EGTA, pH 8.0) containing 20 µg/ml chymostatin, 2 mM PMSF, 10 µM leupeptin, and 1 mM AEBSF. Following SDS-PAGE and transfer to nitrocellulose membranes, blots were sequentially probed with either an anti-Rac1 monoclonal mouse Ab, an anti-Rac2 rabbit polyclonal Ab, and an anti-p38MAPK rabbit polyclonal Ab, followed by HRP-conjugated anti-mouse or anti-rabbit IgG. Proteins were visualized using an ECL detection kit (Amersham Pharmacia Biotech). Bands were scanned and the densities were analyzed by NIH image software (<http://rsb.info.nih.gov/nih-image/>).

Multiple exposures were analyzed to ensure that relative signal intensities measured were in the linear range.

Measurement of NADPH oxidase activity

For quantitative assays, either isoluminol chemiluminescence or a colorimetric assay based on reduction of cytochrome *c* was used to detect reactive oxygen species (8,23). Under these conditions, superoxide dismutase inhibited the chemiluminescence signal by ~97.5% and cytochrome *c* reduction by ~100%. Chemiluminescence in fMLP-stimulated cells was detected as relative luminescence units (RLU) by fast kinetic mode for 100 sec using an Lmax microplate luminometer and SoftMax Pro software (Molecular Devices, Sunnyvale, CA). The rate of cytochrome *c* reduction was measured as V_{max} using SpectraMax340c microplate reader and the SoftMax PRO software (Molecular Devices, Sunnyvale, CA).

Chemotaxis

Neutrophil chemotaxis assays using 1 and 10 μ M fMLP were performed using a modified Boyden chamber (48-well microchemotaxis chamber, Neuro Probes, MD) and 3 μ m diameter polycarbonate filter membranes as described previously (8,15). The number of migrated cells per high power view field (400x) were counted for a minimum of three fields per well, and an average estimation for individual sample was calculated from data of replicate wells. Values were compared relative to the number of migrated cells in the WT group.

Time-lapse video microscopy and motility analysis

Neutrophil motility in response to fMLP stimulation was recorded using a Dunn chemotaxis chamber (24). BM neutrophils in HBSS were allowed to adhere to clean glass coverslips for 15 minutes at 37 C. The coverslips were mounted on the Dunn chamber with a gradient of 0-10 μ M fMLP between the inner and outer wells of the chamber. The chamber was mounted on the microscope stage and the

temperature maintained at 37 °C with a stage heater (Instec Instruments, Boulder, CO). The chamber was allowed to equilibrate for 25 minutes prior to image collection to allow a stable gradient to develop. Images were recorded at 10-second intervals on a Nikon Diaphot 300 microscope with differential interference contrast optics using a SPOT cooled CCD camera. Cell positions were tracked using the particle tracking capabilities in Metamorph 6.1 software (Universal Imaging, Brandywine, PA). Cell trajectories were analyzed using the horizon method (24,25), in which the position of the cell is marked once it reaches a “horizon” at 30 μm from the initial position, and used to define the trajectory of the cell relative to the orientation of the gradient. This methodology can only be applied to cell types that move a significant distance over the time period analyzed, and therefore directional data could not be obtained for *rac2*^{-/-} or Rac1-transduced *rac2*^{-/-} cells. Directionality was evaluated relative to the null hypothesis of uniformity using the Rayleigh test (25). In all cases over 350 cells of each type were analyzed.

Statistical analysis

The two-tailed Student's T test (either paired or unpaired, as indicated) was performed using Microsoft Excel software (Redmond, WA). Statistical comparisons of the distribution of rates of movement between cell types were made using the Wilcoxon-Mann-Witney rank sum test with Kaleidagraph software (Synergy Software, Reading, PA). Oriana software (Kovach Computing Services, Pentraeth, Wales) was used to plot circular histograms and for statistical analysis of directional data.

Results

Expression of recombinant Rac proteins in neutrophils differentiated in vitro

In initial studies, recombinant Rac proteins were expressed in *rac2*^{-/-} neutrophils differentiated *in vitro*. *Rac2*^{-/-} myeloid progenitor cells were transduced with MSCV-based retroviral vectors designed to express Rac1 or Rac2. In preliminary studies using MIEG-based retroviral vectors for transduction followed by *in vitro* differentiation, recombinant Rac proteins were expressed at levels that were three- to six -fold greater than endogenous levels in wild-type neutrophils.² Therefore, subsequent *in vitro* studies utilized the MSCV-pac backbone, which contains a linked antibiotic resistance gene, puromycin-*N*-acetyl-transferase (*pac*) (Fig. 1b), where exogenous Rac proteins were not overexpressed (see below). Vectors included those in which an epitope tag was placed on the amino-terminus of Rac (an HA tag for Rac1 or a FLAG tag for Rac2) as well as those for expression of Rac1 or Rac2 without an epitope tag. Following transduction, bone marrow cells were differentiated *in vitro* with G-CSF and IL-3 with or without puromycin, as described in the Methods, with 80 - 90% morphologically mature neutrophils present after 12 -14 days. In the absence of selection, no differences in expansion or neutrophil differentiation were observed between WT or *rac2*^{-/-} BM that was either mock-transduced or transduced with a control vector containing only the puromycin cassette. There were also no significant differences in expansion or neutrophil differentiation between puromycin-selected WT and *rac2*^{-/-} cells transduced with the control vector containing only the puromycin cassette, or in *rac2*^{-/-} cells transduced with Rac-containing vectors.

To evaluate expression of Rac isoforms in neutrophils differentiated *in vitro*, we performed immunoblotting using antibodies specific for either Rac1 or Rac2 (Fig. 2a). Recombinant Rac proteins were expressed from the MSCV-pac vectors at 60% of endogenous levels, based on densitometric analysis of blots from 4 independent experiments (not shown). Placement of an epitope tag retarded the migration of the recombinant Rac proteins, as expected (Fig. 2a), but did not affect the relative level of expression. Endogenous Rac1 levels in the *in vitro* differentiated *rac2*^{-/-} neutrophils were not significantly increased from wild-type levels (Fig. 2a).

NADPH oxidase activity in wild type and $rac2^{-/-}$ neutrophils differentiated in vitro

Quantitative assessment of NADPH oxidase activity in neutrophils differentiated *in vitro* was performed using a chemiluminescence assay to detect FMLP-induced production of reactive oxidants and the cytochrome *c* reduction assay to measure superoxide production in cells stimulated with phorbol myristate acetate (PMA). $Rac2^{-/-}$ neutrophils had substantially reduced NADPH oxidase activity compared to WT neutrophils (Fig. 2), as previously reported for neutrophils harvested either from the bone marrow storage pool or from peritoneal exudate (8,12,15,26). For both genotypes, there was no significant difference in oxidant production between neutrophils derived from mock-transduced cells compared to puromycin-selected cells transduced with the control MSCV-pac vector (not shown). Expression of either exogenous Rac1 or Rac2 increased NADPH oxidase activity in Rac2-null cells stimulated with either FMLP or PMA. The time course of oxidant production in representative experiments is shown in Fig. 2b and c, and aggregate data is shown in Fig. 2d and e. Of note, Rac derivatives with an epitope tag had a reduced ability to rescue NADPH oxidase activity in $rac2^{-/-}$ neutrophils compared to exogenous Rac proteins lacking a tag, although both epitope- and non-epitope-tagged exogenous Rac proteins were expressed at similar levels (Fig. 2a).

Expression of Rac2 was consistently slightly more effective than exogenous Rac1 in enhancing NADPH oxidase activity in $rac2^{-/-}$ neutrophils (eg. Fig 2b), although the difference in activity between the Rac2- and Rac1-transduced groups did not reach statistical significance. Only partial reconstitution of NADPH oxidase activity was observed even in Rac2-transduced $rac2^{-/-}$ neutrophils, which may reflect the fact that exogenous Rac proteins were expressed at only 60% of wild-type levels using the MSCV-pac vectors (see above). Neutrophils isolated from heterozygous $rac2^{+/-}$ BM, which have one-half the level of Rac2 protein compared to $rac2^{+/+}$ neutrophils, also have reduced superoxide production compared to wild-type neutrophils (8). Similarly, NADPH oxidase activity in $rac2^{+/-}$ neutrophils differentiated *in vitro* as above is reduced by 25% or 50% following PMA or FMLP stimulation, respectively.²

Retrovirus-mediated expression of exogenous Rac1 and Rac2 in neutrophils differentiated in vivo

We next examined whether expression of exogenous Rac1 or Rac2 in *rac2*^{-/-} neutrophils differentiated *in vivo* could reconstitute NADPH oxidase activity and motility. The above results using *rac2*^{-/-} neutrophils differentiated *in vitro* with hematopoietic growth factors indicated that exogenous expression of either isoform improved NADPH oxidase activity, with expression of exogenous Rac2 only slightly more effective than Rac1. GM-CSF or TNF- α treatment of neutrophils isolated from *rac2*^{-/-} mice can partially correct defective NADPH oxidase activity and chemoattractant-induced actin formation (15), raising the question that exposure to pharmacologic concentrations of growth factors during the *in vitro* differentiation process may have influenced these results. Thus, we transplanted Rac-transduced *rac2*^{-/-} bone marrow cells into lethally irradiated *rac2*^{-/-} mice in order to study function of neutrophils produced *in vivo*. Rac derivatives without epitope tags were utilized for these studies.

Initial transplant studies using the MSCV-pac vectors (Fig. 1b) showed that recombinant Rac proteins were expressed at only 5% of wild-type levels in neutrophils produced *in vivo* (not shown). Expression vectors for Rac1 and Rac2 based on the MIEG3 retrovirus (Fig. 1b) were next evaluated. Flow cytometry for EGFP expression was used to select transduced cells by FACS prior to transplantation into lethally irradiated *rac2*^{-/-} recipients. Following hematopoietic recovery, between 60 - 92% of neutrophils were EGFP-positive in all but one mouse (a recipient of MIEG3-Rac1-transduced cells), with most animals having at least 80% EGFP-positive neutrophils. That fewer than 100% neutrophils were EGFP-positive despite sorting for EGFP fluorescence prior to transplantation likely reflects provirus silencing in a subset of transduced repopulating cells, as observed in other studies where transduced BM cells are sorted *ex vivo* prior to transplantation (eg (27)). As shown in a representative immunoblot in Fig. 3a, expression levels of exogenous Rac1 and Rac2 in neutrophils harvested from *rac2*^{-/-} mice receiving transduced marrow were similar to endogenous levels in *rac2*^{+/+} neutrophils. An exception was one recipient of MIEG3-Rac2-transduced BM, in which neutrophil expression of exogenous Rac2 was only 35% of wild-type levels (not shown), which was excluded from the analyses of NADPH oxidase activity and chemotaxis below.

NADPH oxidase activity of $rac2^{-/-}$ neutrophils produced in vivo following transduction for expression of Rac1 or Rac2

We examined NADPH oxidase activity in neutrophils harvested from $rac2^{-/-}$ mice hematopoietically reconstituted with Rac-transduced $rac2^{-/-}$ BM cells and which had 60 - 92% EGFP-positive neutrophils. As shown in Fig. 3, expression of exogenous Rac2 in $rac2^{-/-}$ neutrophils restored fMLP- and PMA-stimulated activity to wild type levels. However, increased expression of Rac1 resulted in a much smaller increase in oxidant production, and the time course of fMLP-stimulated oxidant production resembled that of $rac2^{-/-}$ neutrophils, lacking the rapid onset of oxidant production characteristic of fMLP-stimulated $rac2^{+/+}$ neutrophils (Fig. 3b). Taken together, these results indicate that the Rac2 isoform is essential for normal NADPH oxidase activity in neutrophils produced *in vivo*, and that increased expression of Rac1 cannot compensate for its absence in $rac2^{-/-}$ neutrophils.

NADPH oxidase activity in $rac2^{-/-}$ neutrophils expressing Rac1 and Rac2 derivatives chimeric for the polybasic domain

Rac1 and Rac2 have the greatest sequence divergence in the polybasic domain adjacent to the prenylation site (Fig. 1a). To determine whether this domain could mediate isoform specificity in NADPH oxidase activity in neutrophils produced *in vivo*, we utilized cDNAs in which the sequence encoding the polybasic domain in Rac1 was replaced with the corresponding sequence from the human Rac2 (referred to as Rac1-2), and vice versa (referred to as Rac2-1) (11) (Fig. 1a). These cDNAs were cloned into MIEG3 retroviral vectors (Fig. 1b), which were used to transduce $rac2^{-/-}$ BM cells. Lethally irradiated $rac2^{-/-}$ mice were transplanted as above with transduced cells sorted for EGFP expression. EGFP-positive neutrophils in transplanted mice ranged from 75 - 100%, and expression levels of Rac1-2 and Rac2-1 proteins were similar to endogenous Rac1 and Rac2 (Fig. 4a). The mobility of the chimeric Rac proteins was also similar to endogenous Rac, consistent with normal prenylation of the chimeras. Of note, the polybasic domain appears to be the dominant epitope recognized by the Rac1 and Rac2

antibodies used in this study, since the Rac1-2 protein was detected by the Rac2 antibody and the Rac2-1 protein was detected by the Rac1 antibody (Fig. 4a).

Analysis of NADPH oxidase activity in neutrophils harvested from *rac2*^{-/-} mice transplanted with Rac1-2 or Rac2-1-transduced marrow cells showed that the polybasic domain is sufficient to determine isoform specificity (Fig. 4b, c). fMLP- or PMA-stimulated NADPH oxidase activity in Rac1-2-expressing *rac2*^{-/-} neutrophils was similar to that observed for wild-type neutrophils, including the time course of oxidant production, whereas expression of Rac2-1 produced only a very small, if any, increase in NADPH oxidase activity. Interestingly, NADPH oxidase activity in *rac2*^{-/-} neutrophils expressing exogenous Rac1 was greater than in *rac2*^{-/-} cells expressing Rac2-1 (compare Fig. 3 and Fig. 4).

Chemotaxis in Rac-transduced rac2^{-/-} neutrophils

We also analyzed chemotaxis in *rac2*^{-/-} neutrophils and Rac-transduced *rac2*^{-/-} neutrophils harvested from bone marrow. In Boyden chamber assays, expression of either the Rac2 isoform or the Rac1-2 derivative containing the polybasic domain of Rac2 restored chemotaxis of *rac2*^{-/-} neutrophils towards fMLP (Fig. 5). However, migration of *rac2*^{-/-} neutrophils expressing either Rac2-1 or additional Rac 1 was similar to control *rac2*^{-/-} cells (Fig. 5).

We used time-lapse video microscopy to directly observe the motility of BM neutrophils migrating in a linear gradient of fMLP established in a Dunn (24) chemotaxis chamber. As previously described and as shown in Fig. 6, Supplementary Fig.1, and accompanying movies in Supplementary Figs. 2 and 3, few *rac2*^{-/-} cells displayed directed movement (<7.5% moved at greater than 2 μ m/min, vs. >40% of WT cells, p <0.01, Wilcoxon rank sum test, N >350). Expression of Rac2 was effective in restoring chemotaxis in *rac2*^{-/-} cells, whereas expression of Rac1 did not appreciably rescue motility (6% >2 μ m/min, similar to *rac2*^{-/-}, p >0.05, Wilcoxon test) (Fig. 6a, Supplementary Fig. 1 and movies in Supplementary Figs. 4 and 5; 33% >2 μ m/min). Expression of Rac1-2 was also effective in restoring

motility in *rac2*^{-/-} cells (Fig. 6b; 21% >2 μ m/min), whereas Rac2-1 was ineffective (9% >2 μ m/min, not statistically different from *rac2*^{-/-}, $p>0.05$, Wilcoxon test) (see also Supplementary Figs. 1, 6, and 7).

Analysis of the directionality of BM neutrophil chemotaxis (Fig. 6c) showed that expression of Rac2 and Rac1-2 rescued directed migration of *rac2*^{-/-} ($p<0.01$ relative to null hypothesis of uniformity (non-directional migration), $N=30$, Rayleigh test (25)). Migration was aligned with the orientation of the gradient (mean vector relative to gradient (0°): Rac2, 15°; Rac1-2, 2°). Neither *rac2*^{-/-} nor Rac1-transduced *rac2*^{-/-} cells moved sufficiently far during the period of analysis to reach the 30 μ m “horizon” that would have permitted their directionality to be analyzed. Movement of some Rac2-1-expressing *rac2*^{-/-} cells, however, was sufficient for analysis. Remarkably, these Rac2-1 expressing cells clearly lacked directionality in their movement ($p>0.05$, Rayleigh test, $N=25$) (Fig. 6c; see also Supplementary Fig. 1).

Discussion

Genetic deletion of the hematopoietic-specific Rac2 GTPase produces a variety of defects in different blood cell lineages, suggesting that this isoform plays a non-redundant role in regulating blood cell functions despite concomitant expression of the highly homologous Rac1 isoform (15,20,28). Comparison of Rac1 and Rac2 activation in chemoattractant-stimulated *rac2*^{+/+}, *rac2*^{+/-}, and *rac2*^{-/-} murine neutrophils suggests that these two isoforms have both differential activation and signaling profiles, with four-fold more Rac2-GTP detected compared to Rac1-GTP in fMLP-treated *rac2*^{+/+} neutrophils (8). Furthermore, NADPH oxidase activity is intact in *rac1*^{-/-} neutrophils, which also exhibit only a modest impairment in chemotaxis compared to *rac2*^{-/-} neutrophils (17). Taken together, these observations support the concept that the role of each isoform in regulating neutrophil functions is distinct. The current study was designed to directly address this hypothesis. Wild type murine neutrophils have similar amounts of Rac1 and Rac2, and total cellular levels of Rac are diminished by 2-fold in *rac2*^{-/-} neutrophils (8). We found that increasing cellular Rac levels by retrovirus-mediated expression of Rac2 in *rac2*^{-/-} neutrophils *in vivo* restored NADPH activity and chemotaxis, whereas expression of additional Rac1 only partially corrected these defects. Moreover, isoform specificity could be determined solely by sequences derived from the C-terminal polybasic domain that is adjacent to the prenylation site. A chimeric Rac1-2 protein in which the Rac1 polybasic domain was replaced with that of human Rac2 functioned in a manner similar to Rac2 in reconstituting the NADPH oxidase and chemotaxis in *rac2*^{-/-} neutrophils, whereas expression of an analogous Rac2-1 chimera did not.

A variety of molecular mechanisms could potentially account for distinct roles of Rac1 and Rac2. Although these two isoforms have an identical amino acid sequence in the effector domain, differences in the flexibility of this loop identified in molecular modeling studies, presumably due to long-range effects of divergent residues, may result in differential binding to Rac guanine nucleotide exchange factors or downstream targets (9). In addition, differences in a proline-rich region just N-terminal to the polybasic domain determine relative interactions with the adaptor protein Crk (29) and those at positions 90, 107, 147, and 151 influence the ability of the Rho-inactivating toxin, *Escherichia coli* cytotoxic necrotizing

factor 1, to preferentially degrade Rac1 compared to other Rac isoforms (30). However, the results of the current study indicate that the polybasic domain (residues 183 - 188) is sufficient to determine the relative ability of Rac 1 and 2 to regulate superoxide production and chemotaxis in neutrophils.

The Rac polybasic domain has previously been shown to be an important determinant in a variety of cellular processes. In fibroblast and epithelial cell lines, the polybasic domain directs localization of Rac1 and Rac2 (upon their activation or when expressed in excess of RhoGDI) to either the plasma membrane or to perinuclear endosomal membranes, respectively (10). Deletion of the polybasic domain in Rac2 impairs its biologic activities in neutrophils, which in conjunction with the CAAX motif directs membrane localization (31). The Rac1 polybasic domain contains a nuclear localization signal and Rac1 expression in the nucleus of cultured fibroblasts and epithelial cells has been reported, which may regulate Rac1 levels via proteasome-mediated degradation (10,32,33). The polybasic domain can also influence interactions with proteins that regulate Rac-GTP levels or are downstream targets of Rac. For example, Rac1 binds to and activates the serine-threonine kinase PAK1 more efficiently than Rac2, with the converse observed in chimeric proteins in which the polybasic domains were swapped (11). Phosphoinositide 5-kinase activation in epithelial cell lines is dependent on the C-terminal polybasic domain of Rac1, to which it binds more efficiently compared to the Rac2 polybasic domain (29). Co-immunoprecipitation of Rac1 with the formin/diaphanous related protein FHOS is also mediated by its polybasic domain (34). Differences in the analogous hypervariable domain in the C-terminus of mammalian Ras isoforms have also been shown to determine specifically in localization and interaction partners (35). Hence, the non-redundant role of Rac2 in regulating neutrophil responses could reflect polybasic domain-mediated differences in the localization of activated Rac to subcellular membrane compartments or micro domains, the relative affinities with proteins that regulate Rac activation or serve as downstream targets, or a combination of these factors.

Although expression of Rac2 or Rac1-2 was required for full reconstitution of superoxide production in *rac2*^{-/-} neutrophils *in vivo*, expression of exogenous Rac1 did produce small improvements. In *rac2*^{-/-} neutrophils, Rac1 is already activated to a three-fold greater extent compared to wild-type

neutrophils (8), and the current results suggest that increased expression of this isoform can improve phorbol ester- or fMLP-stimulated NADPH oxidase activity in *rac2*^{-/-} neutrophils. Rac1 was also recently shown to be the predominant form of Rac in human monocytes, where it was suggested to function as the main isoform for superoxide production elicited by PMA and other agonists (36). Rac1 translocates to monocyte membranes in response to PMA, fMLP or opsonized zymosan, and co-immunoprecipitates with the p47^{phox} and p67^{phox} NADPH oxidase subunits upon opsonized zymosan stimulation (36). Of note, murine neutrophils with a combined deficiency of both Rac1 and Rac2 have extremely low superoxide production (28).

Also noteworthy is that expression of the Rac2-1 chimera containing the Rac1 polybasic domain did not increase NADPH oxidase activity in *rac2*^{-/-} neutrophils, in contrast to the small improvements seen with expression of exogenous Rac1. In addition, *rac2*^{-/-} neutrophils expressing Rac2-1 exhibited disoriented cell motility. The underlying basis for these observations remains to be determined. However, the different responses when expressing exogenous Rac1 compared to Rac2-1 are not easily understood in terms of a mechanism for isoform specificity that is based solely on polybasic domain-directed localization of activated Rac.

Placement of an epitope tag on proteins is a useful strategy for distinguishing an exogenous protein from endogenous. Although not the focus of this report, it is of interest that placement of either an HA or FLAG tag on the N-terminus of Rac1 and Rac2, respectively, blunted their ability to enhance NADPH oxidase activity in *rac2*^{-/-} neutrophils. This suggests that these tags impaired Rac activation and/or downstream signaling. To our knowledge, this is the first time epitope tagging of a small GTPase has been reported to interfere with its function, although most studies typically involve overexpression in heterologous cell systems where such effects might be easily missed.

Results from this and our previous (8,12,15) studies indicate that Rac2 is a key regulator of oxidant production and motility. The assembled NADPH oxidase complex includes activated Rac, which binds to p67^{phox} and also likely to flavocytochrome *b*₅₅₈ (2,37). In the cell free NADPH oxidase system, recombinant prenylated Rac1 and Rac2 have equal potential for activating NADPH oxidase using purified

flavocytochrome b_{558} and recombinant cytosolic *phox* proteins (38). Although NADPH oxidase activity elicited by opsonized zymosan is unaffected in *rac2*^{-/-} neutrophils, these cells exhibit decreased superoxide production in response to fMLP, PMA or IgG-opsonized particles (8,12,15). The agonist-selective defects in NADPH oxidase activity in *rac2*^{-/-} neutrophils suggest that Rac2 regulates upstream events and/or is more efficiently incorporated into the oxidase complex compared to Rac1 in response to these agonists. The first scenario is supported by the observation that Rac2-null neutrophils have other functional defects in response to agonists that are associated with reduced NADPH oxidase activity (8,12,15). The parallel effects of exogenous Rac1, Rac2, and chimeric Rac proteins on chemotaxis and superoxide production by *rac2*^{-/-} neutrophils in this study is also consistent with roles in shared signaling pathways.

Our observations also support a critical role for Rac2 in cell orientation in chemotaxis. We previously showed that *rac2*^{-/-} cells, in addition to their impaired ability to move, are not polarized in the direction of the chemotactic gradient (15). We show here that Rac1-2, as well as Rac2 itself, fully rescued the ability of cells to move and, moreover, to properly orient their motility in a chemotactic gradient. Rac2-1 cells displayed a greater defect in chemotaxis in Boyden chamber assays than the frequency and speed of migrating Rac2-1 cells might predict, but the discrepancy can easily be explained by the remarkably disoriented nature of their motility. This is consistent with the accepted critical role for Rac in chemotactic signaling pathways (39-41), and illuminates possible isoform-specific roles in this process that have not previously been recognized. The Rac GTPases are proposed to be a component of a positive feedback loop involving the GTPase and phosphatidylinositol 3-kinase that is important for establishment of cell polarity and the maintenance of a “front-ness” signal at the leading edge (39,40). Although we were unable to definitively determine whether Rac1 expressing cells showed directed migration (due to their poor motility and consequent failure to reach the 30 μ m horizon required for the analysis), the disoriented nature of the motile response displayed by Rac2-1 expressing cells is highly suggestive of a critical role for factors that specifically interact with the Rac2 polybasic domain in establishing cell

polarity and orientation. Our results suggest the need for more work to determine interactions that specify distinct roles for Rac1 and Rac2 in regulating the cytoskeleton in hematopoietic cells.

While this manuscript was in preparation, a study by Filippi and colleagues (42) reported findings generally consistent with those described here, with a notable difference with respect to reconstitution of neutrophil motility. Similar to our results, migration of fMLP-stimulated *rac2*^{-/-} neutrophils in Boyden chambers was reconstituted by expression of Rac2. However, rescue by a Rac1-2 chimera additionally required replacement of a glycine at position 150 with aspartic acid, the residue at the corresponding position in Rac2 (42). This contrasts with our findings, where expression of a Rac1-2 chimera was sufficient to reconstitute fMLP-stimulated chemotaxis in *rac2*^{-/-} neutrophils (Fig. 5, 6). However, the study by Filippi et al used the murine Rac2 polybasic domain, which differs from the human Rac2 sequence used here, in having a proline instead of an alanine at position 188 (Fig. 1a). Other factors that may have contributed to the different results are that Filippi et al used neutrophils differentiated *in vitro* and exogenous Rac proteins that were HA-tagged and relatively overexpressed (42).

Filippi and coworkers also reported differences in localization of EGFP-tagged Rac proteins in murine neutrophils, which may contribute to their different functions (42). In resting cells, EGFP-Rac1 was dispersed compared to a more central cytoplasmic and perinuclear localization for EGFP-Rac2. Upon fMLP stimulation both forms were also detected at more peripheral locations, with Rac1 co-localizing with cortical actin and Rac2 being somewhat more interior. Moreover, in fMLP-stimulated *rac2*^{-/-} neutrophils, EGFP-Rac1 was poorly organized, suggesting that there may be crosstalk between the two Rac isoforms. Since deficient F-actin formation is a notable feature of fMLP-stimulated *rac2*^{-/-} neutrophils (15), Filippi et al proposed that Rac1 distribution may be correlated to F-actin organization and that Rac1 dysfunction in *rac2*^{-/-} neutrophils might contribute to their abnormal chemotaxis. We are currently undertaking studies to examine Rac1 and Rac2 localization in neutrophils isolated from bone marrow or peripheral blood. In preliminary studies on unstimulated murine neutrophils stained with Rac1 and Rac2 antibodies or expressing small amounts of exogenous EGFP-Rac1 or EGFP-Rac2, both

isoforms were distributed diffusely in the cytosol.³ These results are consistent with studies on resting human neutrophils, where Rac2 is cytosolic and in a complex with RhoGDI (43), but differ from the localization described by Filippi and coworkers (see above) (42). However, Rac proteins were relatively overexpressed in the latter studies, possibly exceeding Rho-GDI binding capacity (10), and also studied in neutrophils differentiated *in vitro* using relatively high concentrations of growth factors. Neither we³ nor Filippi et al (42) detected a significant pool of nuclear Rac1 in neutrophils.

In conclusion, these results establish that Rac2 plays a non-overlapping role with Rac1 to regulate neutrophil chemotaxis and NADPH oxidase activity, and demonstrate that the C-terminal polybasic domain is sufficient for conferring this specificity. Future studies will address underlying mechanisms that discriminate between Rac1 and Rac2, which may include differences in subcellular targeting as well as binding to interacting regulatory or downstream target proteins.

Acknowledgments

We thank Natalie Stull for taking care of mice we used here, and Shari Upchurch and Kim Cunningham for managing preparation of this manuscript. We also thank Wade Clapp and Lawrence Quilliam for review of the manuscript and helpful discussions. This work was supported by a National Institutes of Health Grants PO1HL69974 (MCD, SJA), RO1HL45635 (MCD), RO1 AI 35947 (UK) and the Riley Children's Foundation (MCD).

References

1. Dinauer, M. (2003) in *Nathan and Oski's Hematology of Infancy and Childhood* (Nathan, D., Orkin, S., Ginsburg, D., and Look, A., eds) Vol. 1, 6th Ed., pp. 923-1010, 2 vols., W.B. Saunders Company, Philadelphia
2. Dinauer, M. (2003) *Curr Opin Hematol* **10**, 8-15
3. Etienne-Manneville, S., and Hall, A. (2002) *Nature* **420**, 629-635
4. Didsbury, J., Weber, R., Bokoch, G., Evans, T., and Snyderman, R. (1989) *J Biol Chem* **264**, 16378-16382
5. Shirsat, N., Pignolo, R., Kreider, B., and Rovera, G. (1990) *Oncogene* **5**, 769-772
6. Moll, J., Sansig, G., Fattori, E., and van der Putten, H. (1991) *Oncogene* **6**, 863-866
7. Haataja, L., Groffen, J., and Heisterkamp, N. (1997) *J Biol Chem* **272**, 20384-20388
8. Li, S., Yamauchi, A., Marchal, C., Molitoris, J., Quilliam, L. A., and Dinauer, M. (2002) *J Immunol*, 5043-5051
9. Haeusler, L. C., Blumenstein, L., Stege, P., Dvorsky, R., and Ahmadian, M. R. (2003) *FEBS Lett* **555**, 556-560
10. Michaelson, D., Silletti, J., Murphy, G., D'Eustachio, P., Rush, M., and Philips, M. R. (2001) *J Cell Biol* **152**, 111-126.
11. Knaus, U. G., Wang, Y., Reilly, A. M., Warnock, D., and Jackson, J. H. (1998) *J Biol Chem* **273**, 21512-21518
12. Kim, C., and Dinauer, M. (2001) *J Immunol* **166**, 1223-1232
13. Williams, D., Tao, W., Yang, F., Kim, C., Gu, Y., Mansfield, P., Levine, J., Petryniak, B., Darrow, C., Harris, C., Jia, B., Zheng, Y., Ambruso, D., Lowe, J., Atkinson, S., Dinauer, M., and Boxer, L. (2000) *Blood* **96**, 1646-1654
14. Ambruso, D. R., Knall, C., Abell, A. N., Panepinto, J., Kurkchubasche, A., Thurman, G., Gonzalez-Aller, C., Hiester, A., deBoer, M., Harbeck, R. J., Oyer, R., Johnson, G. L., and Roos, D. (2000) *Proc Natl Acad Sci U S A* **97**, 4654-4659

15. Roberts, A., Kim, C., Zhen, L., Lowe, J., Kapur, R., Petryniak, B., Spaetti, A., Pollock, J., Borneo, J., Bradford, G., Atkinson, S., Dinauer, M., and Williams, D. (1999) *Immunity* **10**, 183-196
16. Heyworth, P., Bohl, B., Bokoch, G., and Curnutte, J. (1994) *J Biol Chem* **269**, 30749-30752
17. Glogauer, M., Marchal, C. C., Zhu, F., Worku, A., Clausen, B. E., Foerster, I., Marks, P., Downey, G. P., Dinauer, M., and Kwiatkowski, D. J. (2003) *J Immunol* **170**, 5652-5657
18. Knaus, U. G., Heyworth, P. G., Kinsella, B. T., Curnutte, J. T., and Bokoch, G. M. (1992) *J Biol Chem* **267**, 23575-23582
19. Hawley, R., Lieu, F., Fong, A., and Hawley, T. (1994) *Gene Ther* **1**, 136-138
20. Yang, F. C., Kapur, R., King, A. J., Tao, W., Kim, C., Borneo, J., Breese, R., Marshall, M., Dinauer, M. C., and Williams, D. A. (2000) *Immunity* **12**, 557-568
21. Bjorgvinsdottir, H., Ding, C., Pech, N., Gifford, M., Li, L., and Dinauer, M. (1997) *Blood* **89**, 41-48
22. Zhen, L., King, A., Xiao, Y., Chanock, S., Orkin, S., and Dinauer, M. (1993) *Proc Natl Acad Sci USA* **90**, 9832-9836
23. Dahlgren, C., and Karlsson, A. (1999) *J Immunol Methods* **232**, 3-14.
24. Zicha, D., Dunn, G., and Jones, G. (1997) *Methods in Molecular Biology* **75**, 449-457
25. Mardia, K. V., and Jupp, P. E. (1999) *Directional Statistics*, 2nd Ed., John Wiley & Sons, Chichester, UK
26. Kim, C., Marchal, C. C., Penninger, J., and Dinauer, M. C. (2003) *J Immunol* **171**, 4425-4430
27. Sadat, M., Pech, N., Saulnier, S., LeRoy, B., Hossle, J., Grez, M., and Dinauer, M. (2003) *Hum Gene Ther* **14**, 651-666
28. Gu, Y., Filippi, M. D., Cancelas, J. A., Siefring, J. E., Williams, E. P., Jasti, A. C., Harris, C. E., Lee, A. W., Prabhakar, R., Atkinson, S. J., Kwiatkowski, D. J., and Williams, D. A. (2003) *Science* **302**, 445-449

29. van Hennik, P. B., ten Klooster, J. P., Halstead, J. R., Voermans, C., Anthony, E. C., Divecha, N., and Hordijk, P. L. (2003) *J Biol Chem* **278**, 39166-39175
30. Pop, M., Aktories, K., and Schmidt, G. (2004) *J Biol Chem* **279**, 35840-35848
31. Tao, W., Filippi, M.-D., Bailey, J., Atkinson, S. J., Connors, B., Evan, A., and Williams, D. A. (2002) *Blood* **100**, 1679-1688
32. Williams, C. L. (2003) *Cell Signal* **15**, 1071-1080
33. Lanning, C. C., Daddona, J. L., Ruiz-Velasco, R., Shafer, S. H., and Williams, C. L. (2004) *J Biol Chem* Published online on August 10, 2004
34. Westendorf, J. J. (2001) *J Biol Chem* **276**, 46453-46459
35. Hancock, J. F. (2003) *Nat Rev Mol Cell Biol* **4**, 373-384
36. Zhao, X., Carnevale, K. A., and Cathcart, M. K. (2003) *J Biol Chem* **278**, 40788-40792
37. Diebold, B., and Bokoch, G. (2001) *Nat Immunol* **2**, 211-215
38. Heyworth, P., Knaus, U., Settleman, J., Curnutte, J., and Bokoch, G. (1993) *Molecular Biology of the Cell* **4**, 1217-1223
39. Devreotes, P., and Janetopoulos, C. (2003) *J Biol Chem* **278**, 20445-20448
40. Weiner, O. D., Neilsen, P. O., Prestwich, G. D., Kirschner, M. W., Cantley, L. C., and Bourne, H. R. (2002) *Nat Cell Biol* **4**, 509-513
41. Xu, J., Wang, F., Van Keymeulen, A., Herzmark, P., Straight, A., Kelly, K., Takuwa, Y., Sugimoto, N., Mitchison, T., and Bourne, H. R. (2003) *Cell* **114**, 201-214
42. Filippi, M. D., Harris, C. E., Meller, J., Gu, Y., Zheng, Y., and Williams, D. A. (2004) *Nat Immunol* **5**, 744-751
43. Abo, A., Webb, M., Grogan, A., and Segal, A. (1994) *Biochem. J.* **298**, 585-591

Footnotes

¹ The abbreviations used are PAK, p21-activated kinase; PAC, puromycin-*N*-acetyl-transferase; IRES, internal ribosome entry sequence; EGFP, enhanced green fluorescent protein; SCF, stem cell factor; MDGF, megakaryocyte-derived growth factor; AEBSF, 4-(2-Aminoethyl)-benzenesulfonylfluoride.HCl; Ab, antibody; PMA, phorbol myristate acetate

² A. Yamauchi and M. Dinauer, unpublished data.

³ S. Atkinson, A. Yamauchi and M. Dinauer, unpublished data

Figure Legends

Figure 1. C-terminus of Rac proteins and retroviral vectors for expression of Rac.

A. Sequence alignment of the C-terminus of wild type Rac1, Rac2, and derivatives. Hyphens indicate sites where amino acid residues are identical to wild type murine Rac1, whereas differences are as indicated. The polybasic domain is indicated by a rectangle. Mu, murine; hu, human. Note that the entire murine Rac1 and human Rac1 amino acid sequence are identical. B. MSCV-PAC and MIEG3 retroviral vectors. The genes between long terminal repeats (LTR) are shown. PGK, phosphoglyceroyl kinase; pac, puromycin-*N*-acetyl-transferase; H, HA epitope tag; F, Flag epitope tag, IRES, internal ribosome entry site; EGFP, enhanced green fluorescent protein.

Figure 2. Rac expression and NADPH oxidase activity in neutrophils differentiated *in vitro*.

After transduction with MSCV-pac retrovirus vectors, or mock-transduction, murine bone marrow cells were cultured with IL-3 and G-CSF for differentiation *in vitro* as described in Methods. MSCV-pac retrovirus-transduced cells were selected in puromycin. Wild type, *rac2*^{-/-}, or *rac2*^{-/-} cells expressing exogenous Rac proteins are as indicated. Emp, empty (MSCV-Pac lacking a Rac cDNA); R1, Rac1; HR1, HA-tagged Rac1; R2, Rac2; FR2, Flag-tagged Rac2. A. Immunoblot of extracts prepared from *in vitro*-differentiated neutrophils, using anti-Rac1, anti-Rac2 or anti-p38MAPK, as indicated. Note that epitope tagged Rac proteins migrated slightly slower than untagged Rac proteins, and Rac1-transduced *rac2*^{-/-} cells contain both endogenous and exogenous Rac1. Representative of 4 experiments. B, C. Representative time course of ROS production by *in vitro* differentiated neutrophils detected by chemiluminescence (for fMLP-stimulated cells, B) or reduction of cytochrome *c* (PMA-stimulated superoxide production, C). RLU, relative luminescence units. mOD, optical density (x 10⁻³). D, E. Quantitative analysis of NADPH oxidase activity in *in vitro* differentiated neutrophils. Superoxide dismutase- inhibitable luminescence (integrated RLU over 100 sec) is shown for fMLP-elicited ROS production (D). The maximal rate of superoxide dismutase- inhibitable cytochrome *c* reduction (V_{max}) is shown for PMA-elicited superoxide production. Means ± SEM are shown; N = 9 for WT and *rac2*^{-/-}

controls; N =3 -6 for Rac-transduced *rac2^{-/-}* cells. ‡ p < 0.02 (vs *rac2^{-/-}* emp), ‡‡ p < 0.005 (vs *rac2^{-/-}* emp), # p <0.01 (vs R2, paired test, n = 3). ** p = 0.057 (vs *rac2^{-/-}* emp). p values except R2 vs FR2 are based on unpaired student's t-test.

Figure 3. Rac expression and NADPH oxidase activation of neutrophils isolated from WT, *rac2^{-/-}*, and *rac2^{-/-}* mice transplanted with Rac1- or Rac2- transduced BM.

Rac2^{-/-} BM was transduced with MIEG3 retroviral vectors for expression of either Rac1 or Rac2, sorted for EGFP-positive cells, and transplanted into *rac2^{-/-}* mice as described in Methods. Immunoblots and NADPH oxidase assays were performed on freshly isolated neutrophils from transplanted mice. *Rac2^{-/-}* control mice were transplanted with untransduced *rac2^{-/-}* BM. Wild type, *rac2^{-/-}*, or *rac2^{-/-}* cells expressing exogenous Rac proteins are as indicated, and abbreviations are as in Fig. 2. A. Immunoblot of extracts prepared from BM neutrophils, using anti-Rac1, anti-Rac2 or anti-p38MAPK, as indicated. Representative of 3 experiments. Note that the antibody for Rac2 has some cross reactivity with Rac1, (15) which accounts for the faint band in Rac1-transduced *rac2^{-/-}* extracts probed for Rac2. B, C. Representative time course of neutrophil ROS production detected by chemiluminescence (for fMLP-stimulated cells, B) or reduction of cytochrome *c* (PMA-stimulated superoxide production, C). RLU, relative luminescence units. mOD, optical density (x 10⁻³). The fraction of EGFP-positive neutrophils for Rac1- and Rac2-transduced *rac2^{-/-}* neutrophils was 84% and 92%, respectively. D, E. Quantitative analysis of neutrophil NADPH oxidase activity. Superoxide dismutase- inhibitable luminescence (integrated RLU over 100 sec) is shown for fMLP-elicited ROS production (D). The maximal rate of superoxide dismutase- inhibitable cytochrome *c* reduction (V_{max}) is shown for PMA-elicited superoxide production. Means ± SEM are shown. N = 14 and 8 for WT and *rac2^{-/-}* controls, respectively. N = 3 for Rac-transduced *rac2^{-/-}* neutrophils. * p < 0.05 (vs *rac2^{-/-}*), ** p < 0.00005 (vs *rac2^{-/-}*), # p < 0.02 (vs WT), ### p < 0.0005 (vs WT). p values are based on unpaired student's t-test.

Figure 4. Rac expression and NADPH oxidase activation of neutrophils isolated from WT, *rac2*^{-/-}, and *rac2*^{-/-} mice transplanted with Rac1-2- or Rac2-1- transduced BM.

Experimental design and abbreviations are as described in Fig. 3. A. Immunoblot of extracts prepared from freshly isolated neutrophils, using anti-Rac1, anti-Rac2 or anti-p38MAPK, as indicated.

Representative of 4 experiments. B, C. Representative time course of neutrophil ROS production detected by chemiluminescence (for fMLP-stimulated cells, B) or reduction of cytochrome *c* (PMA-stimulated superoxide production, C). RLU, relative luminescence units. mOD, optical density (x 10⁻³). The fraction of EGFP-positive neutrophils for Rac1-2- and Rac2-1-transduced *rac2*^{-/-} neutrophils was 83% and 80%, respectively. D, E. Quantitative analysis of neutrophil NADPH oxidase activity.

Superoxide dismutase- inhibitable luminescence (integrated RLU over 100 sec) is shown for fMLP-elicited ROS production (D). The maximal rate of superoxide dismutase- inhibitable cytochrome *c* reduction (V_{max}) is shown for PMA-elicited superoxide production. Means ± SEM are shown. N = 14 and 8 for WT and *rac2*^{-/-} controls, respectively. N= 3–5 for Rac-transduced *rac2*^{-/-} cells. * p < 0.0002 (vs *rac2*^{-/-}), **p < 0.00001 (vs *rac2*^{-/-}). p values are based on unpaired student's t-test.

Figure 5. Chemotaxis of neutrophils isolated from WT, *rac2*^{-/-}, and *Rac2*^{-/-} transplanted with Rac-transduced BM.

Experimental design and abbreviations are as described in Fig. 3 and 4. Chemotaxis assays performed on freshly isolated neutrophils, using a modified Boyden chamber in response to 1 μM or 10 μM fMLP as described in Methods. The ligand was loaded in the lower wells and the cells (2 x 10⁵) were loaded in upper wells separated by a 3 μm pore size filter membrane, followed by incubation at 37 °C for 45 min. The number of migrated cells was subsequently counted by microscopic examination. Results are expressed as the percentage of migrated cells per field compared to WT control neutrophils. Means ± SEM are shown. *p < 0.002 (vs *rac2*^{-/-}); **p < 0.0005 (vs *rac2*^{-/-}). p values are based on unpaired student's t-test (n = 3).

Figure 6. Videomicroscopy analysis of fMLP-induced motility in neutrophils isolated from WT, *rac2*^{-/-}, and *Rac2*^{-/-} transplanted with Rac-transduced BM.

Freshly isolated neutrophils were exposed to a linear gradient of 0-10 μ M fMLP in a Dunn chemotaxis chamber and the positions of cells were recorded at 10-second intervals over a 15-minute period. See also accompanying movies S2-6, and supplementary Fig. S1. A. Histogram of the mean speed distribution of WT, *rac2*^{-/-}, and Rac1 and Rac2 transduced *rac2*^{-/-} cells. Data were derived from three independent experiments. B. Histogram of the mean speed distribution of WT, *rac2*^{-/-} and Rac1-2 and Rac2-1 transduced *rac2*^{-/-} cells. Data were derived from three independent experiments. C. Circular histograms showing the distributions of cell trajectories of WT cells or *rac2*^{-/-} cells transduced with Rac2, Rac1-2 or Rac2-1 relative to the orientation of the gradient (0°). Plots show the mean direction and 95% confidence limit for the trajectories where there was a significant non-uniform distribution. Each plot shows a representative experiment from a total of three independent experiments with similar results.

Figure 1

A

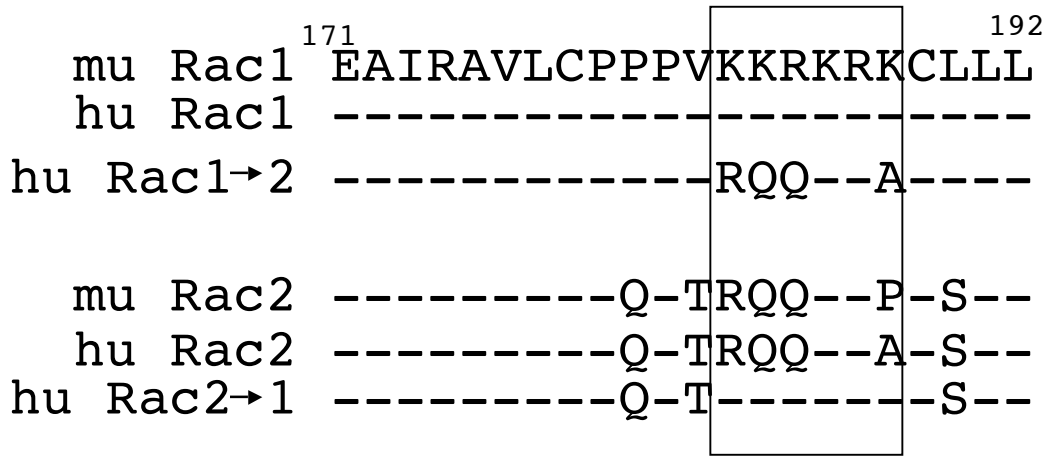
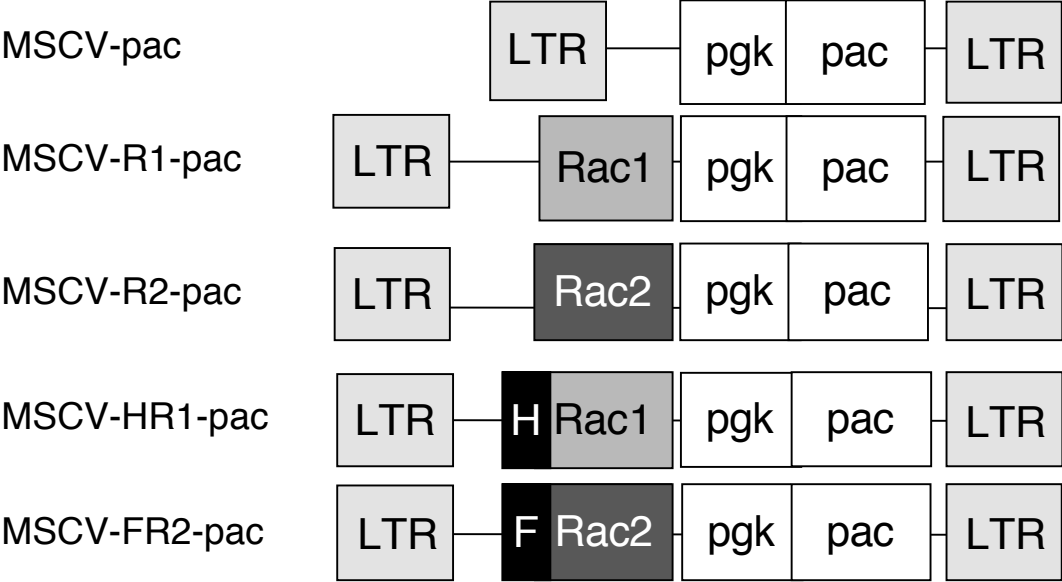


Figure 1B

MSCV-pac retrovirus vectors



MIEG3 retrovirus vectors

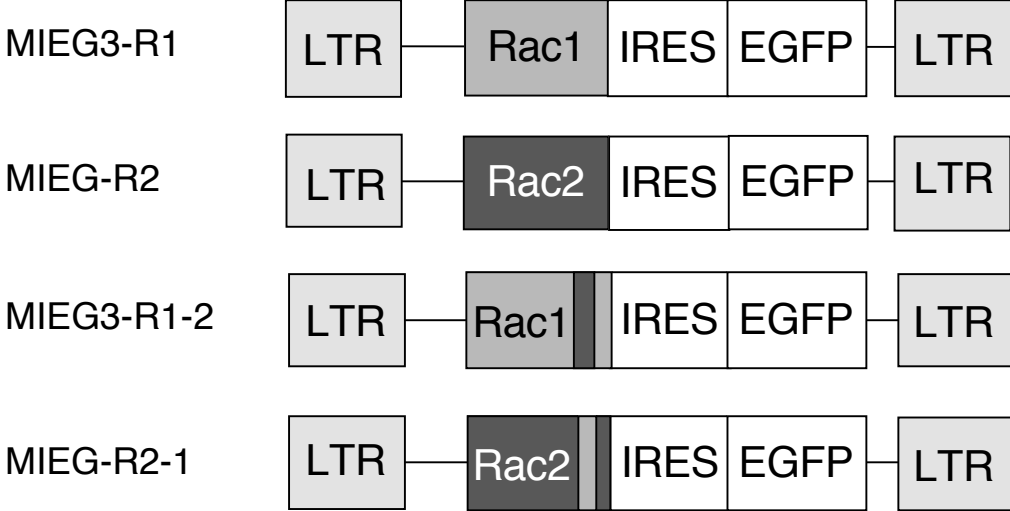
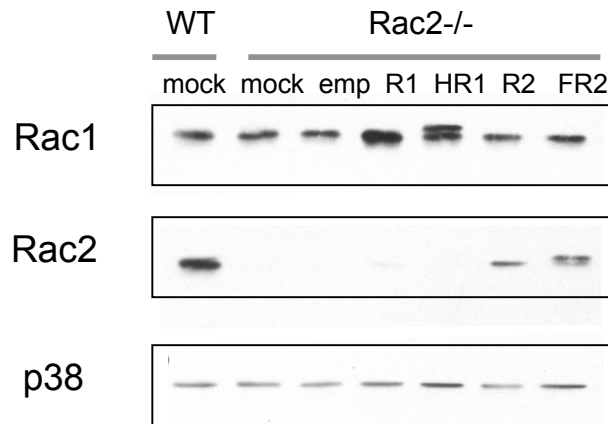
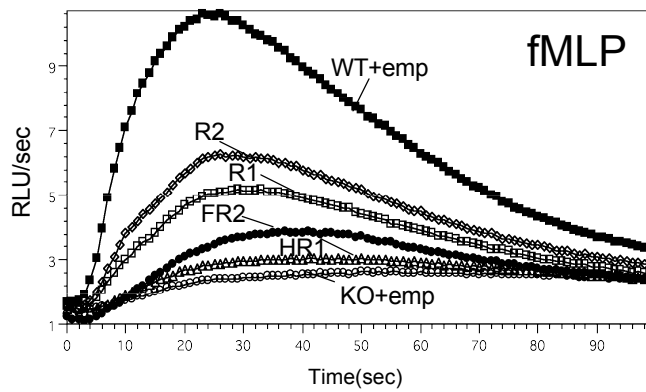


Figure 2

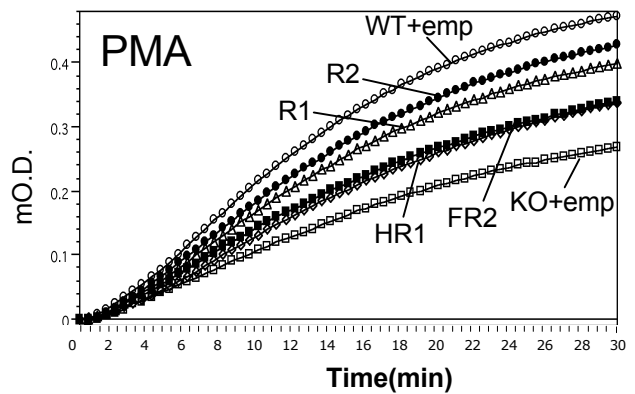
A



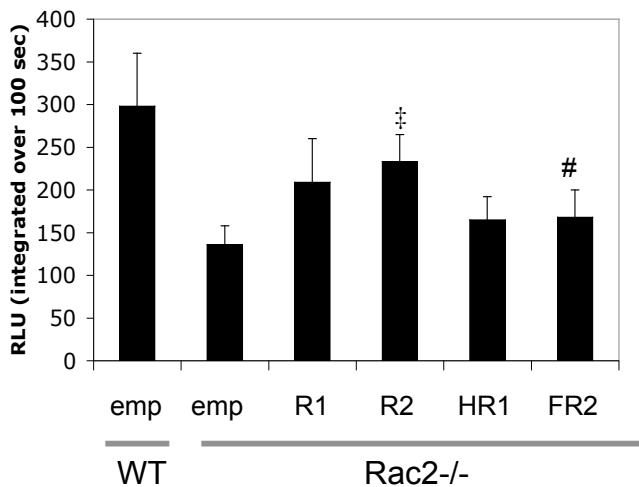
B



C



D



E

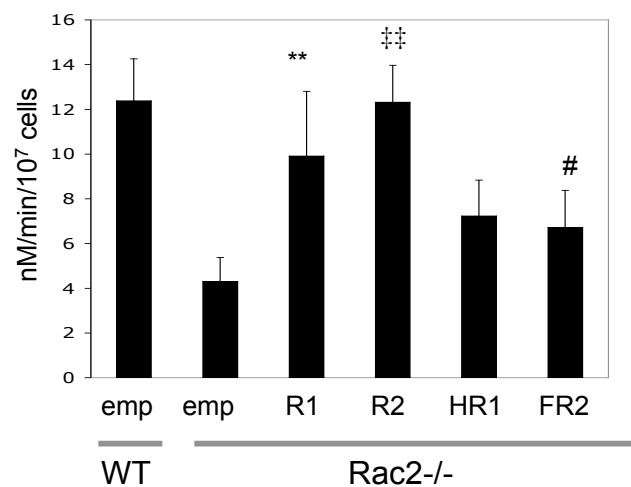
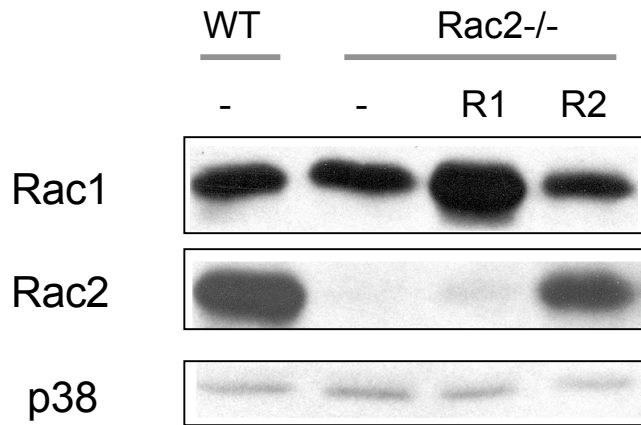
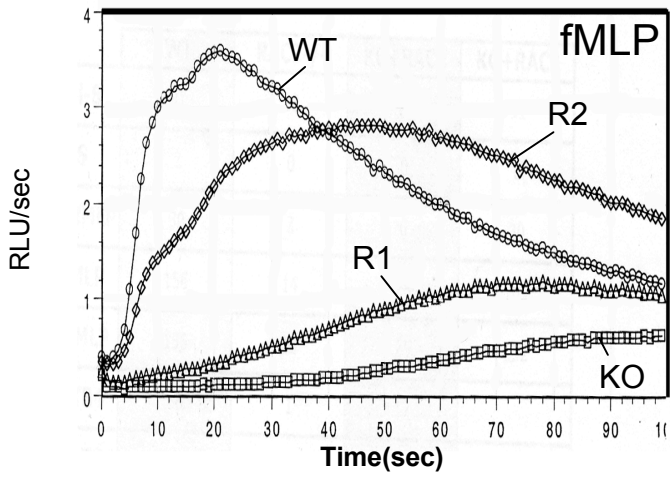


Figure 3

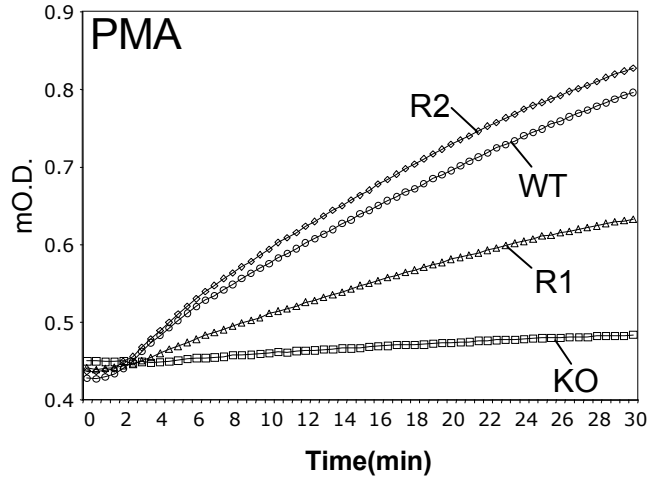
A



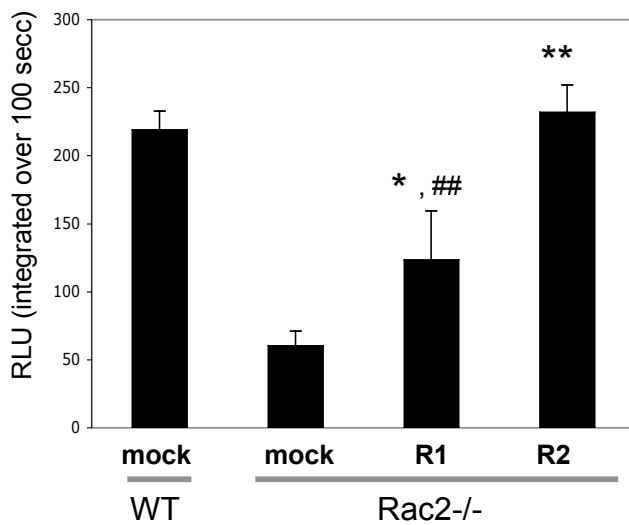
B



C



D



E

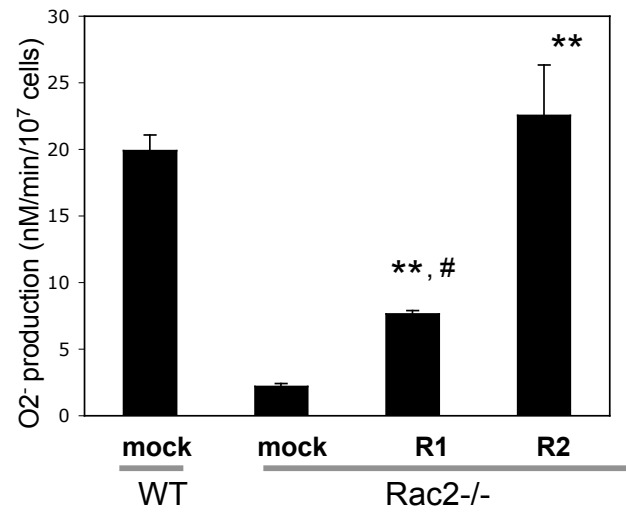


Figure 4

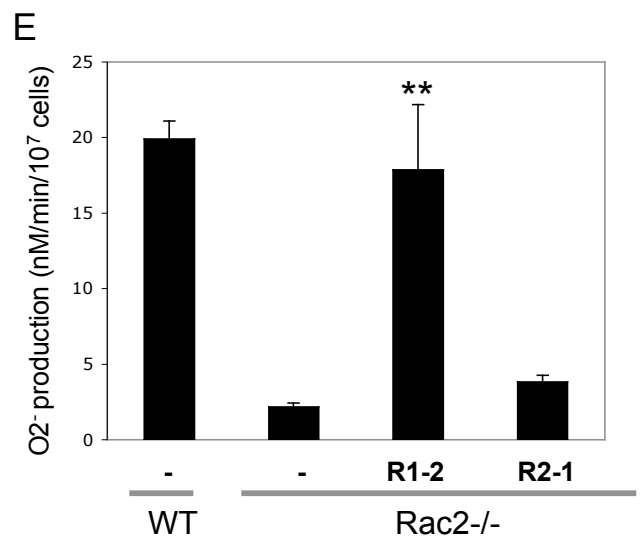
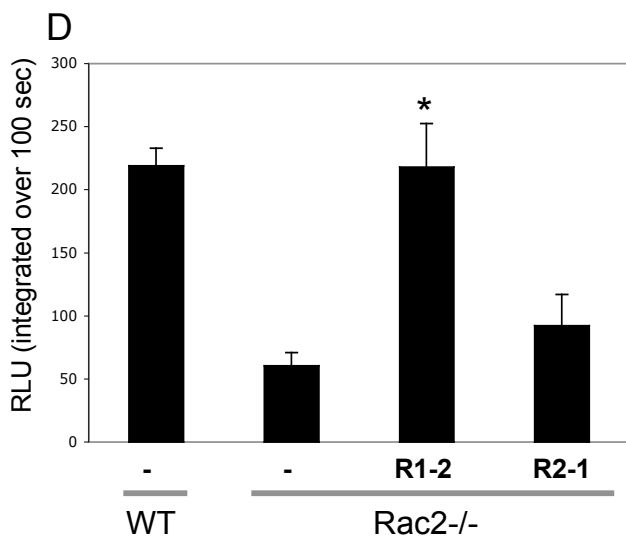
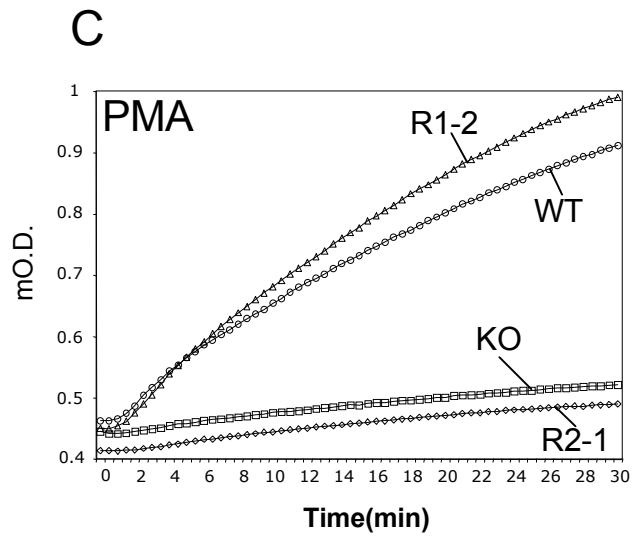
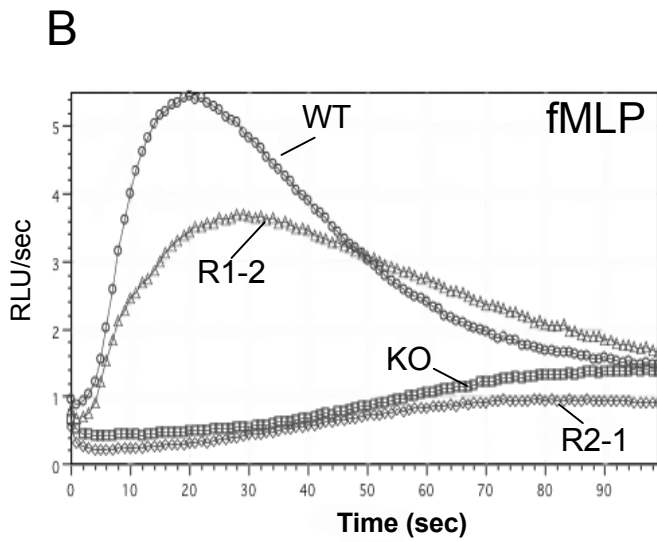
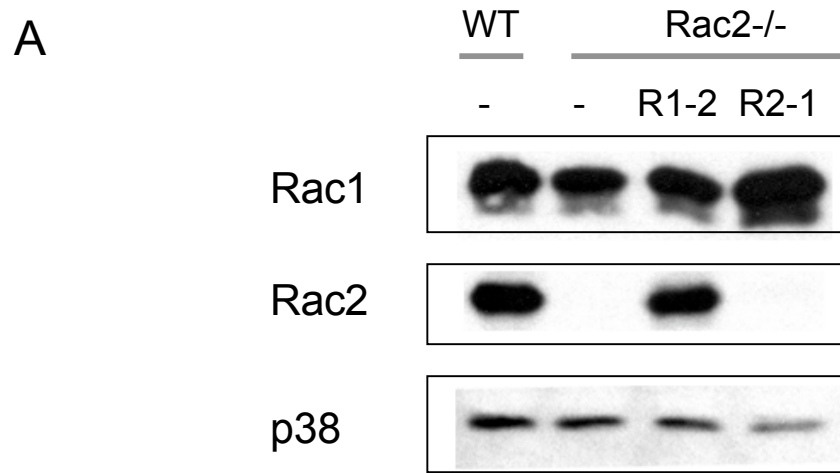


Figure 5

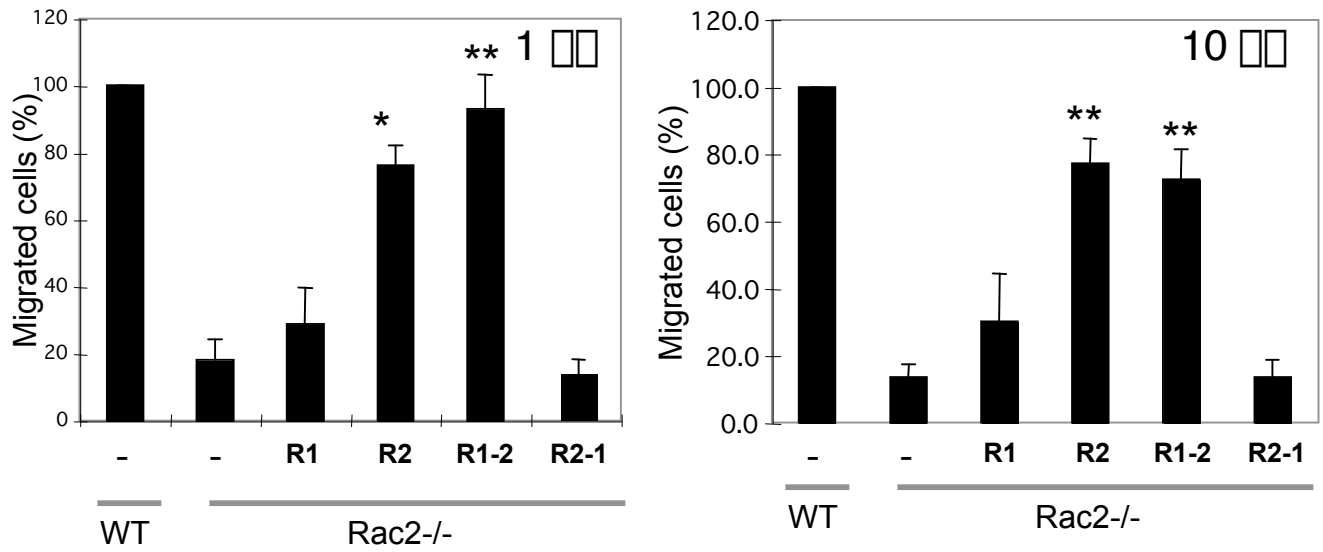
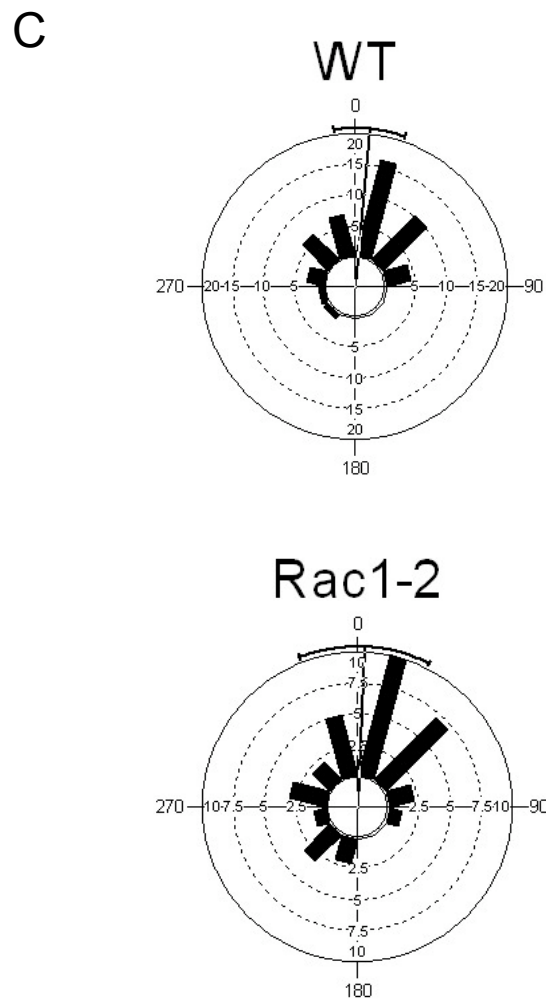
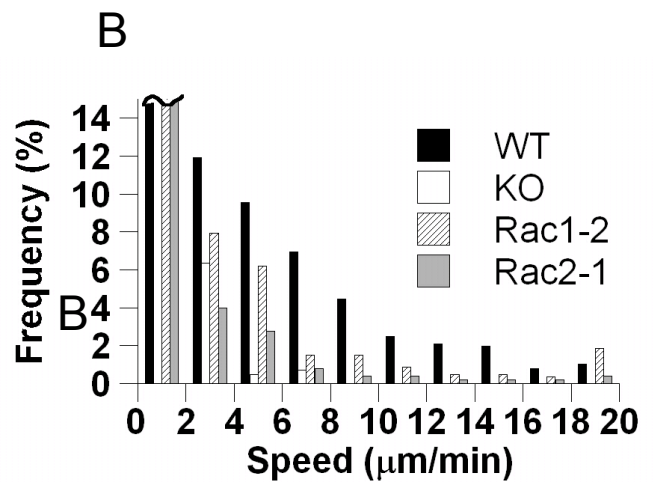
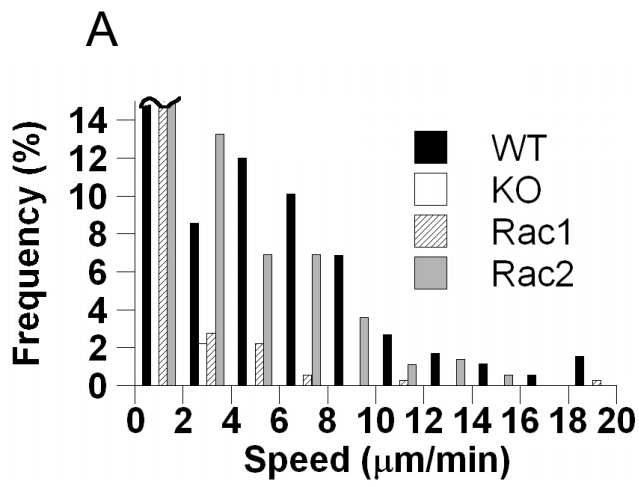


Figure 6



Supplementary Figure S1

Representative tracks for individual WT, *rac2*^{-/-} or *rac* transduced *rac2*^{-/-} BM neutrophils moving in a gradient of 0-10 μ M fMLP. The plots show the tracks of 15 randomly chosen cells from representative experiments relative to the cell's initial position at the first time point analyzed. The concentration of fMLP increases from left to right. Data are representative of three independent experiments. Note that although the distance traveled by several of the Rac1-2-transduced cells shown in Fig. S1 was greater than for the Rac2-transduced cells shown, overall there was no difference in the speed frequency distribution between these two groups (See Fig. 6A).

Supplementary Figures S2-S7

Representative time-lapse movies of murine neutrophils migrating in a gradient of 0-10 μ M fMLP, with the concentration of fMLP increasing from left to right across the field. Movies are 120x real time, field of view is 230x230 μ m.

S2. Wild type

S3. *Rac2*^{-/-}

S4. Rac1 expressing *rac2*^{-/-} cells.

S5. Rac2 expressing *rac2*^{-/-} cells.

S6. Rac1-2 expressing *rac2*^{-/-} cells.

S7. Rac2-1 expressing *rac2*^{-/-} cells.

Supplementary Figure 1

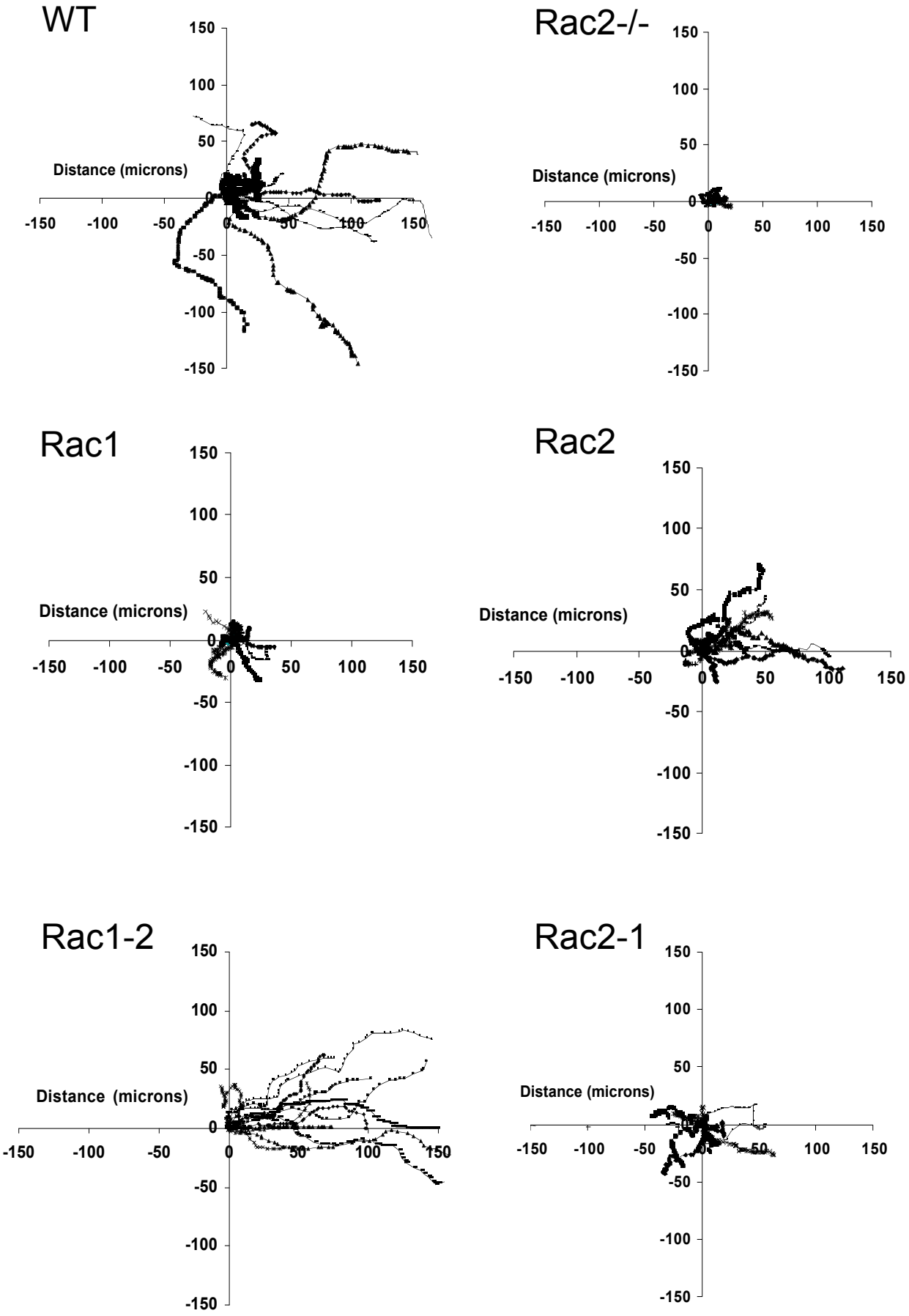


Figure S2. WT motility



Figure S3. KO motility



Figure S4. KO+R1 motility



Figure S5. KO+R2 motility



Figure S6. KO+R1-2 motility

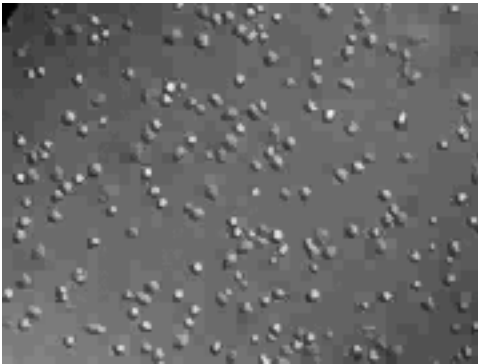


Figure S7. KO+R2-1 motility

